SCIENCE CHINA
Technological Sciences

• Article •

September 2016 Vol.59 No.9: 1328–1339
doi: 10.1007/s11431-016-6090-6

Mesh stiffness evaluation of an internal spur gear pair with tooth profile shift

CHEN ZaiGang[1*], ZHAI WanMing[1], SHAO YiMin[2] & WANG KaiYun[1]

[1] *State Key Laboratory of Traction Power, Southwest Jiaotong University, Chengdu 610031, China;*
[2] *State Key Laboratory of Mechanical Transmission, Chongqing University, Chongqing 400030, China*

Received February 23, 2016; accepted April 27, 2016

Tooth profile shift will change the thickness of gear teeth and a part of geometrical parameters of a gear pair, thus influencing its mesh stiffness and consequently the dynamic performances. In this paper, an analytical mesh stiffness calculation model for an internal gear pair in mesh considering the tooth profile shift is developed based on the potential energy principle. Geometrical representations of the tooth profile shift are firstly derived, and then fitted into the analytical tooth stiffness model of gears. This model could supply a convenient way for mesh stiffness calculation of profile shifted spur gears. Then, simulation studies are conducted based on the developed model to demonstrate the effects of tooth profile shift coefficient on the tooth compliances and the mesh stiffness of the internal spur gear pair. The results show that tooth profile shift has an obvious influence on the mean value, amplitude variation and phase of the mesh stiffness, from which it can be predicted that the dynamic response of an internal gear transmission system will be affected by the tooth profile shift.

mesh stiffness, tooth profile shift, internal gear, gear transmission, tooth compliance

Citation: Chen Z G, Zhai W M, Shao Y M, et al. Mesh stiffness evaluation of an internal spur gear pair with tooth profile shift. Sci China Tech Sci, 2016, 59: 1328–1339, doi: 10.1007/s11431-016-6090-6

1 Introduction

Internal gear pair is a key element in many mechanical transmission systems, such as the planetary gear set which has a wide engineering application due to its advantages of compactness, reduced noise and vibrations, as well as high efficiency et al. This is the reason why it has attracted so much attention from plenty of researchers on its static and dynamic performance, especially its compliance and mesh stiffness which act as one of the inherited internal excitations to the gear transmission system. Hidaka et al. [1] studied the displacement of the sun gear and the ring gear in a planetary gear transmission system, and latter they [2] established an analytical model based on the work achieved by Karas [3] and an finite element model (FEM) to obtain the deformation of a ring gear tooth along line of action (LOA) which is evaluated by the bending moment, shearing force and Hertzian contact using an approximate trapezoid-type tooth profile instead of the involute profile. Chen and Shao [4] extended their previous work [5] on the mesh stiffness calculation method of external spur gear pair based on the potential energy theory to the calculation of internal/ring gear tooth deformation. Based on the analytical calculation model of gear mesh stiffness, they [6,7] further improved their proposed model to be capable of obtaining the mesh stiffness of internal gear pairs with thin-rimmed ring gear for investigation on planetary gear dynamic performance. Satoshi et al. [8] employed FE model to study the rim deformation and stress of a thin-rimmed internal spur

*Corresponding author (email: zgchen@home.swjtu.edu.cn)

gear supported by pins. With a near-field semi-analytical technique and a far-field FEM, Kahraman et al. [9] developed a deformable body dynamic model to study the influence of the gear rim thickness and the number of planets on the gear stress. Although the thin rim will affect the dynamic performance of the internal/ring gear set, the internal/ring gear is also assumed to be rigid in the present paper as many published papers did [10−14], which is reasonable when the ring gear rim is thick enough. Lei et al. [15] reviewed and summarized a number of literatures about condition monitoring and fault diagnosis of planetary gearboxes.

Mesh stiffness variation of gear pairs including external and internal gears is one of the main excitations inherited by the gear transmissions due to the periodic change in the number of gear teeth in mesh and the moving contact position of gear teeth along tooth profile. Although the finite element model (FEM) of a gear pair enables the calculation of mesh stiffness, it requires the mesh refinement and expensive computational cost. As an alternative method, analytical calculation models show well agreement with the FEMs with less computation time [5,16]. Thus, analytical methods for gear mesh stiffness calculation have drawn a wide attention from researchers worldwide.

As early as in 1940s, Weber [17] calculated analytically the mesh stiffness of spur gear pairs. Cornell [18] derived the compliance of the spur gear teeth based on the Weber's model by adding a improved fillet/foundation compliance based on the O'Donnell's work [19]. Based on Cornell's work, Omar et al. [20] obtained the mesh stiffness of spur gear pair with tooth root crack failure, and then the vibration features are compared numerically and experimentally. A mesh stiffness calculation model of a spur gear pair was developed by Yang and Lin [21] based on the potential energy method. By considering the effect of shear mesh stiffness, Tian et al. [22−23] and Wu et al. [24] refined the model developed by Yang and Lin, which was further improved by Chen and Shao [5] with taking the fillet/foundation deflections into consideration and applied to the cracked gear tooth, where the model is capable of dealing with the situation that tooth root circle deviates from the base circle. This improved model was then modified by Mohammed et al. [25] with changing the area shape of the removed material corresponding to the tooth crack. Based on the potential energy principle, Liang et al. [26,27] derived the analytical formulations for mesh stiffness calculation of planetary gear transmissions where both the external and the internal gears were included. Chen and Shao [28] proposed a general mesh stiffness calculation model which can deal with the effect of the tooth profile deviations. Wang et al. [29] extended the model proposed in [5,28] to involve the tooth profile deviations along tooth width, such as the lead crown relief. In these public literatures, effect of the tooth profile shift on the mesh stiffness of gear pairs was ignored.

Under many circumstances, reasonable design of profile shift for a gear pair, including both external and internal gear pairs, is always employed for undercut prevention, center distance adjustment, interference elimination, specific sliding equalization, and tooth bending fatigue life equalization et al. [30−32]. They are manufactured by moving the cutter to or away from the gears to be cut. The gear tooth profile shift has been defined in many standards and literatures, such as ISO [33], AGMA [30] and DIN [34] standards, and the corresponding gear dimension calculation formulas with shifted profile can be found in these literatures. Some parameters of the gears with tooth profile shift will be changed compared with the ones without tooth profile shift, such as radius of tip and root circles, tooth thickness. While for profile shifted gear pairs, a part of its geometric parameters are also likely to be changed, such as the center distance, contact ratio, working pitch diameter and working pressure angle. These variations in the geometric parameters of gears and gear pairs caused by tooth profile shift are likely to change the tooth stiffness and mesh stiffness of the gear pairs, thus leading to the variation of the load sharing and the load carrying capacity. Ristivojević et al. [35] studied the load carrying capacity of the spur gear tooth with and without tooth profile shift, where it was found that the pitch point position affected greatly by the tooth profile shift has a great impact on the tooth load carrying capacity. Marimuthu and Muthuveerappan [36] attempted to find the optimum profile shifts for asymmetric normal contact ratio and high contact ratio gear drives where the objective is to make the maximum tooth fillet stresses of the pinion and the gear to be equal. Abderazek et al. [37] investigated the optimal values of profile shift coefficients for involute spur and helical gears by using a differential evolution algorithm with aim at balancing specific sliding coefficients. Rajesh et al. [38] carried on some analysis of load sharing and bending strength for altered toothsum gears where the tooth profile shift had a great impact on the performance. While for the effect of tooth profile shift coefficient on the mesh stiffness, there has few papers published. Shiau et al. [39] calculated analytically the mesh stiffness of external spur gear pairs with tooth profile shift and investigated the nonlinear dynamics of a multi-gear train. Ma et al. [40] analyzed the effect of the profile modification on the mesh stiffness of an external gear pair with tooth profile shift, and they [41] also carried on some studies on the dynamic responses of external profile shifted gear pair with tooth root crack.

It is noticed from the public literature that there is limited work on the effect of gear tooth profile on the mesh stiffness, especially for the internal gear pairs. Actually, the tooth profile shift coefficient has a great impact on the mesh stiffness, including not only the magnitude, but also the shape and the phase, thus resulting in the possibility of a dynamic performance variation of the gear transmission train. In this paper, an analytical calculation model for mesh stiffness of an internal gear pair with shifted tooth profile is

established based on the previous work in refs. [4,5,26,27] with the potential energy principle. The proposed model enables revealing the effect of the tooth profile shift coefficient on the mesh stiffness of an internal gear pair.

This paper is organized as follows: Reviews on the previous literatures about the research work on gear tooth profile shift and gear mesh stiffness calculation method are carried out in the segment of introduction. Then, an analytical mesh stiffness formulation of an internal gear pair with tooth profile shift is derived in section 2 which is followed by calculated results and discussion in section 3. Finally, conclusions will be drawn in section 4.

2 Analytical mesh stiffness formulation of a profile shifted internal spur gear pair

2.1 Geometric relationship of profile shifted internal gear pairs

Figure 1 shows the schematic of the profile shifted gear teeth. It can be seen that when the profile shift coefficient x is positive, the gear tooth will become thicker at the position with the same radius than the standard gear tooth (x=0), and the working segment of the involute curve profile will move far away from the center of the gear. While for a gear with a negative profile shift coefficient, an inverse phenomenon can be observed. Correspondingly, the central angle between the radius through the initial point of the involute curve and the center line of the gear tooth will vary with the profile shift coefficient, which can be calculated as

$$\alpha_2' = \alpha_2 + \Delta\alpha_2, \tag{1}$$

where the symbol α_2' denotes the central angle with gear tooth profile shift, α_2 the central angle of the standard gear tooth, and $\Delta\alpha_2$ the variation of the central angle due to the gear tooth profile shift. They can be calculated by

$$\alpha_2 = 0.5\pi / z_1 + \tan\alpha_0 - \alpha_0, \tag{2}$$

$$\Delta\alpha_2 = 2x_1 \tan\alpha_0 / z_1, \tag{3}$$

where z_1 is the number of the gear teeth, α_0 the pressure angle of the rack cutter, and x the profile shift coefficient. An internal gear with shifted tooth profile which is not shown here can be also analyzed similarly as the profile shifted external gear teeth illustrated in Figure 1.

When a gear pair with tooth profile shifted is in mesh, its center distance may be varied. Internal gear pairs in mesh with different profile shift coefficient are displayed in Figure 2. It can be seen that the variations of the center distance and the pitch point of the gear pair will be determined by the summation of its profile shift coefficients. When the summation of the profile shift coefficients of the gear pair is

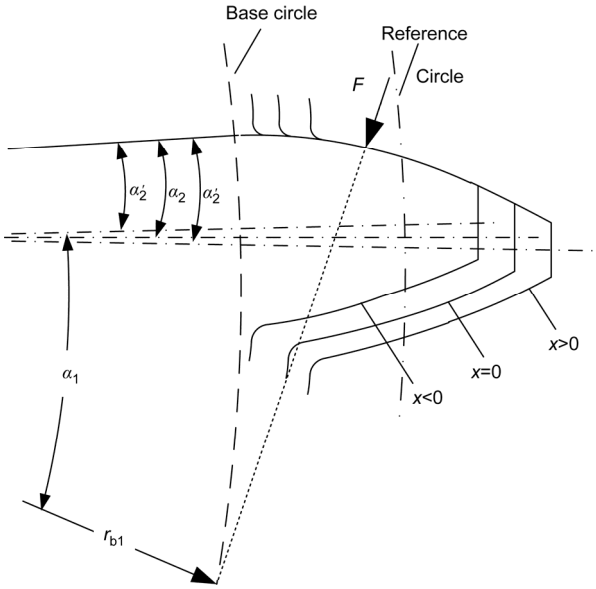

Figure 1 Schematic for external gear teeth with different profile shift coefficient.

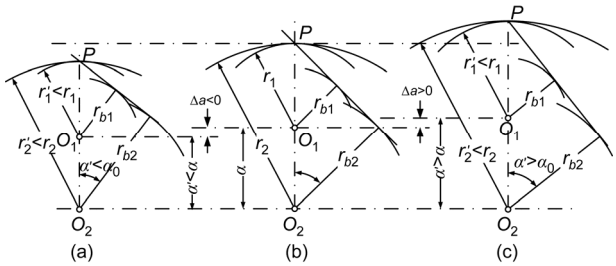

Figure 2 Schematic of internal gear pair mesh: (a) $x_2-x_1<0$, (b) $x_2-x_1=0$, (c) $x_2-x_1>0$.

equal to zero, the center distance a, the working pressure angle α_0 and the radius of the pitch circle r_i (i=1 for external gear and i=2 for internal gear) will not vary compared to the gear pair without profile shift. This case is represented in Figure 2(b). On the other aspect, the center distance a', the working pressure angle α' and the radius of the pitch circle r_i' will become smaller when the summation of the profile shift coefficients is negative (see Figure 2 (a)), while they will enlarge when the summation is positive (see Figure 2(c)).

Formulas of gear geometrical parameters can be found in many literatures for both standard and tooth profile shifted gears or gear pairs [30,33–34]. Some calculation formulas for these parameters related to the tooth profile shift are going to be employed in the following contents. When the involute tooth profiles of an internal gear pair are shifted, the mesh angle α' is likely to be changed. It can be calculated as [30,33–34]

$$\mathrm{inv}\alpha' = 2\tan\alpha_0\left(\frac{x_2 - x_1}{z_2 - z_1}\right) + \mathrm{inv}\alpha_0, \tag{4}$$

where, the symbol α_0 is the reference pressure angle; x_i, z_i (i=1 for external and 2 for internal gears) stand for the tooth profile shift coefficient and the number of gear teeth, respectively. 'inv' denotes the involute function being defined as

$$\mathrm{inv}\alpha = \tan\alpha - \alpha. \tag{5}$$

Additionally, the center distance maybe varies if the gear tooth profile is shifted according to the geometrical relationship shown in Figure 2. It can be calculated by [30,33]

$$a' = m\left(\frac{z_2 - z_1}{2} + y\right), \tag{6}$$

where the letter, y, is the center distance modification coefficient which is calculated by

$$y = \frac{z_2 - z_1}{2}\left(\frac{\cos\alpha_0}{\cos\alpha'} - 1\right). \tag{7}$$

The tip radius of the external and internal gears of the internal gear pair are calculated by [30,33]

$$r_{a1} = m(z_1/2 + h_a + x_1), r_{a2} = m(z_2/2 - h_a + x_2). \tag{8}$$

The root radius of the external and internal gears of the internal gear pair are calculated by [30,33]

$$r_{r1} = r_{a1} - m(2h_a + c), r_{r2} = r_{a2} + m(2h_a + c), \tag{9}$$

where m is the module, r_{ki} (k=a for tip circle and r for root circle; i=1 for external and 2 for internal gears) are the circular tooth thickness at the reference circle and the diameter of the gear, respectively. The symbol h_a is the addendum coefficient and c the tip clearance coefficient.

In summary, some design parameters of the gear such as the tooth thickness, mesh angle, radius of tip circle and root circle, will vary if its tooth profile is shifted. Thus the tooth compliance and the mesh stiffness of the gear pair is likely to be changed which is going to be introduced in the following subsection.

2.2 Mesh stiffness calculation of the internal gear pair

Calculation of gear mesh stiffness analytically could be always achieved by regarding the gear teeth as non-uniform cantilever beams [5,16–22,24–25], which was also employed in our previous published papers with potential energy principle [4–7]. According to the potential energy principle, saying the work done by the external forces is equal to the potential energy stored in the deformation of the flexible body [4,21], the work done by the mesh force applied to a gear tooth along LOA is equal to the potential energy of the flexible deformations of the tooth, involving the bending, shear, and compressive deformations. The work done by the mesh force can be denoted as [4,5,24]

$$U_b = \frac{F^2}{2K_b}, U_s = \frac{F^2}{2K_s}, U_a = \frac{F^2}{2K_a}. \tag{10}$$

The potential energy stored in the tooth flexible deformations can be represented as [4,5,24]

$$U_b = \int_0^d \frac{M^2}{2EI_x}\mathrm{d}x, U_s = \int_0^d \frac{1.2F_b^2}{2GA_x}\mathrm{d}x, U_a = \int_0^d \frac{F_a^2}{2EA_x}\mathrm{d}x, \tag{11}$$

where the symbols U, K are the work done by the mesh force F and the corresponding stiffness of the equivalent spring, and the subscripts b, s, a indicate successively the bending, shear and axial compressive deformations. E and G are the Young modulus and the shear modulus, respectively. The integration boundary d is the effective length of the cantilever beam and x refers to the distance between the concerned cross section of the cantilever beam and that where the mesh force is applied. The moment M, and the component forces F_a and F_b of the mesh force F can be calculated as

$$F_b = F\cos\alpha, \quad F_a = F\sin\alpha, \quad M = F_b x - F_a h. \tag{12}$$

Combining eqs. (1)–(3) yields

$$\frac{1}{K_b} = \int_0^d \frac{(x\cos\alpha - h_f\sin\alpha)^2}{EI_x}\mathrm{d}x, \tag{13-a}$$

$$\frac{1}{K_s} = \int_0^d \frac{1.2\cos^2\alpha}{GA_x}\mathrm{d}x, \tag{13-b}$$

$$\frac{1}{K_a} = \int_0^d \frac{\sin^2\alpha}{EA_x}\mathrm{d}x, \tag{13-c}$$

where the letter h denotes half the tooth thickness corresponding to the contact position. α is the angle between the line perpendicular to the center line of a gear tooth and the line parallel to the mesh force. A and I are the area and area moment of inertia of the tooth cross section, respectively, which are calculated as

$$I_x = \frac{2}{3}Bh_x^3, \quad A_x = 2Bh_x. \tag{14}$$

For more detailed information about the symbols in eqs. (1)–(5), the contents in [5] for external gear pair and in [4] for internal gear are recommended to be referenced, where the standard gears were studied without the effect of tooth profile shift.

More detailed expressions on the analytical mesh stiffness calculation formulations for both external-external and external-internal spur gear pairs without tooth profile shift were derived by Liang et al. [26,27]. For external gears where the gear root circle is smaller than the base circle, the bending stiffness K_b, shear stiffness K_s and axial compressive stiffness K_a are derived in ref. [27] as follows:

$$\frac{1}{K_{\mathrm{b}}}=\frac{[1-\frac{(z-2.5)\cos\alpha_1\cos\alpha_3}{z\cos\alpha_0}]^3-(1-\cos\alpha_1\cos\alpha_2)^3}{2EB\cos\alpha_1\sin^3\alpha_2}$$

$$+\int_{-\alpha_1}^{\alpha_2}\frac{3\{1+\cos\alpha_1[(\alpha_2-\alpha)\sin\alpha-\cos\alpha]\}^2(\alpha_2-\alpha)\cos\alpha}{2EB[\sin\alpha+(\alpha_2-\alpha)\cos\alpha]^3}\mathrm{d}\alpha, \tag{15-a}$$

$$\frac{1}{K_{\mathrm{s}}}=\frac{1.2(1+\upsilon)\cos^2\alpha_1(\cos\alpha_2-\frac{z-2.5}{z\cos\alpha_0}\cos\alpha_3)}{EB\sin\alpha_2}+\int_{-\alpha_1}^{\alpha_2}\frac{1.2(1+\upsilon)(\alpha_2-\alpha)\cos\alpha\cos^2\alpha_1}{EB[\sin\alpha+(\alpha_2-\alpha)\cos\alpha]}\mathrm{d}\alpha, \tag{15-b}$$

$$\frac{1}{K_{\mathrm{a}}}=\frac{\sin^2\alpha_1(\cos\alpha_2-\frac{z-2.5}{z\cos\alpha_0}\cos\alpha_3)}{2EB\sin\alpha_2}+\int_{-\alpha_1}^{\alpha_2}\frac{(\alpha_2-\alpha)\cos\alpha\sin^2\alpha_1}{2EB[\sin\alpha+(\alpha_2-\alpha)\cos\alpha]}\mathrm{d}\alpha. \tag{15-c}$$

While for external gears where the gear root circle is greater than the base circle, the bending, shear and axial compressive stiffness are derived in ref. [27] as follows:

$$\frac{1}{K_{\mathrm{b}}}=\int_{-\alpha_1}^{\alpha_5}\frac{3\{1+\cos\alpha_1[(\alpha_2-\alpha)\sin\alpha-\cos\alpha]\}^2(\alpha_2-\alpha)\cos\alpha}{2EB[\sin\alpha+(\alpha_2-\alpha)\cos\alpha]^3}\mathrm{d}\alpha, \tag{16-a}$$

$$\frac{1}{K_{\mathrm{s}}}=\int_{-\alpha_1}^{\alpha_5}\frac{1.2(1+\upsilon)(\alpha_2-\alpha)\cos\alpha\cos^2\alpha_1}{EB[\sin\alpha+(\alpha_2-\alpha)\cos\alpha]}\mathrm{d}\alpha, \tag{16-b}$$

$$\frac{1}{K_{\mathrm{a}}}=\int_{-\alpha_1}^{\alpha_5}\frac{(\alpha_2-\alpha)\cos\alpha\sin^2\alpha_1}{2EB[\sin\alpha+(\alpha_2-\alpha)\cos\alpha]}\mathrm{d}\alpha, \tag{16-c}$$

where υ is the Poisson's ratio, B the tooth width and E the Young modulus. The angles, namely α_1, α_2, α_3 and α_5, will vary compared with the standard gear if the tooth profile of the gear is shifted. According to eq. (1), the angle α_2 in eqs. (15)–(16) will be replaced by α_2' in the presence of tooth profile shift, which can be calculated as

$$\alpha_2'=\frac{\pi}{2z_1}+\tan\alpha_0-\alpha_0+\frac{2x_1\tan\alpha_0}{z_1}. \tag{17}$$

Then

$$\alpha_3=\arcsin\left(\frac{r_{\mathrm{b1}}\sin\alpha_2'}{r_{\mathrm{r1}}}\right)=\arcsin\left(\frac{\cos\alpha_0\sin\alpha_2'}{1-2(h_{\mathrm{a}}+c-x_1)/z_1}\right), \tag{18}$$

$$\alpha_1=\theta-\alpha_2'+\frac{\sqrt{r_{\mathrm{a2}}^2-r_{\mathrm{b2}}^2}-a'\sin\alpha'}{r_{\mathrm{b1}}}, \tag{19}$$

where the symbol θ is the rotational angle of the external gear relative to the position that the gear teeth is just getting into engagement, and its variation range is calculated as

$$\theta\in\left[0\quad\left(\sqrt{r_{\mathrm{a1}}^2-r_{\mathrm{b1}}^2}-\sqrt{r_{\mathrm{a2}}^2-r_{\mathrm{b2}}^2}+a'\sin\alpha'\right)/r_{\mathrm{b1}}\right], \tag{20}$$

where $r_{\mathrm{b}i}$ (i=1 for external gear and 2 for internal gear) indicates the radius of the base circle of the gears in mesh. Then the contact ratio can be obtained as $CR=\frac{z_1\theta_{\max}}{2\pi}$.

The angle α_5 can be determined by

$$\alpha_5=\sqrt{\left(\frac{r_{\mathrm{r1}}}{r_{\mathrm{b1}}}\right)^2-1}-\alpha_2'=\sqrt{\left[\frac{1-2(h_{\mathrm{a}}+c-x_1)/z_1}{\cos\alpha_0}\right]^2-1}-\alpha_2'. \tag{21}$$

For internal spur gears without profile shift, the bending, shear and axial compressive stiffness have been derived in [26] as

$$\frac{1}{K_{\mathrm{b}}}=\int_{\phi}^{\beta_1}\frac{3\{1+\cos\beta_1[(\beta_2-\beta)\sin\beta-\cos\beta]\}^2(\beta_2-\beta)\cos\beta}{2EB[\sin\beta+(\beta_2-\beta)\cos\beta]^3}\mathrm{d}\beta, \tag{22-a}$$

$$\frac{1}{K_{\mathrm{s}}}=\int_{\phi}^{\beta_1}\frac{1.2(1+\upsilon)(\beta_2-\beta)\cos\beta\cos^2\beta_1}{EB[\sin\beta+(\beta_2-\beta)\cos\beta]}\mathrm{d}\beta, \tag{22-b}$$

$$\frac{1}{K_{\mathrm{a}}}=\int_{\phi}^{\beta_1}\frac{(\beta_2-\beta)\cos\beta\sin^2\beta_1}{2EB[\sin\beta+(\beta_2-\beta)\cos\beta]}\mathrm{d}\beta. \tag{22-c}$$

When the tooth profile of the internal gear is shifted, the angles in eq. (22) will vary relative to its standard form. They can be calculated as

$$\begin{aligned}\beta_2&=\frac{\pi}{2z_2}+\alpha_0-\tan\alpha_0-\frac{2x_2\tan\alpha_0}{z_2},\\ \phi&=\beta_2+\sqrt{\left(\frac{r_{\mathrm{r2}}}{r_{\mathrm{b2}}}\right)^2-1},\\ \beta_1&=\beta_2+\sqrt{\left(\frac{r_{\mathrm{a2}}}{r_{\mathrm{b2}}}\right)^2-1}+\frac{r_{\mathrm{b1}}}{r_{\mathrm{b2}}}\theta.\end{aligned} \tag{23}$$

It should be noted that the radius of the tip circle and root circle of the internal gear are also the functions of the tooth profile shift coefficient. When the gear teeth bending, shear,

and axial compressive stiffness of the internal gear pairs are obtained, the tooth stiffness for both external and internal gears can be derived as [4,5]

$$\frac{1}{K}=\frac{1}{K_{\mathrm{b}}}+\frac{1}{K_{\mathrm{s}}}+\frac{1}{K_{\mathrm{a}}}+\frac{1}{K_{\mathrm{f}}}, \tag{24}$$

where, K is the overall tooth stiffness of a gear tooth, K_{f} denotes the stiffness due to tooth fillet foundation compliance which could be referenced to [4,5,16]. However, some parameters of the external gear such as the central angle θ_{f} and its corresponding arc length S_{f} will be affected if the gear tooth profiles are shifted. They can be obtained as

$$\theta_{\mathrm{f}}=\theta_{\mathrm{f0}}+2x_1\tan\alpha_0/z_1, S_{\mathrm{f}}=S_{\mathrm{f0}}+2r_{\mathrm{b1}}x_1\tan\alpha_0/z_1, \tag{25}$$

where the symbols θ_{f0} and its corresponding arc length S_{f0} represent the central angle and its corresponding arc length of the standard gear. It is noted that the internal gear foundation compliance is not considered in this paper even if it has an obvious impact on the mesh stiffness of a thin-rimed internal gear pair (see refs. [6-7]). When the single tooth stiffness is obtained, the mesh stiffness of the multi-tooth engagement, K_{m}, can be gained by,

$$K_{\mathrm{m}}=\sum_{i=1}^{N}1/\left(\frac{1}{K_i^{\mathrm{e}}}+\frac{1}{K_i^{\mathrm{i}}}+\frac{1}{K_i^{\mathrm{h}}}\right), \tag{26}$$

where, N is the number of tooth pairs in mesh, and K_i^j (j=e for external gear teeth, i for internal gear teeth, and h for Hertzian contact deformation) the stiffness. Actually, eq. (26) indicates only the gear pairs without manufacturing errors which have proved that it has great effect on the mesh stiffness and dynamic responses of the gear system [28]. However, the internal gear pairs investigated in this paper are assumed to be ideal without any errors. Based on the method for the Hertzian contact stiffness calculation of external gear pairs presented in refs. [21], Liang et al. [26] derived the Hertzian contact stiffness calculation formulas of an internal gear pair, which has the same form as that of external gear pairs. By using the same method presented in refs. [21,26], the Hertzian contact stiffness formulas for the profile shifted internal gear pairs is derived here which has the same expression as that in [21,26],

$$\frac{1}{K^{\mathrm{h}}}=\frac{4(1-\upsilon^2)}{\pi EB}. \tag{27}$$

3 Results and discussion

Based on the extended analytical calculation model of internal spur gear pair developed in section 2, a specified gear pair is employed to demonstrate the effect of tooth profile shift. The main design parameters of the internal gear pair are given in Table 1. Three groups of tooth profile shift coefficients of the internal gear pair are assumed and shown in Table 2. These profile shift coefficients are selected based on the design requirements such as prevention of undercut, elimination of teeth interference, and keeping necessary tooth top land thickness. The profile shift coefficient of the external gear varies from –0.33 to 0.99 for the three cases, but changing the coefficient of the internal gear to alter the center distance of the internal gear pair. Case I in Table 2 indicates that the distance between the centers of the external and internal gears keeps unchanged relative to the its standard case, namely the summation of the profile shift coefficients is equal to zero. While case II and III show the conditions that the summations of the profile shift coefficients are positive (x_2–x_1=0.21) and negative (x_2–x_1=–0.19), respectively. In case II, the centers of the external and internal gears departure from each other compared with its standard form, while they are approaching with each other in case III. In case II (or III), the summation of the profile shift coefficient keeping as constant indicates the center distance of the gear pair is constant. In addition, the contact ratios of the given gear pairs are also calculated and given in Table 2. It can be seen that the contact ratio for any one of the three cases will decrease as the increase in the tooth profile shift coefficient.

Some calculated results are displayed in Figures 3–9. It should be noted that the x-axis label for these figures is the rotational angle of the external gear, and the angular position being equal to zero corresponds to the gear teeth con-

Table 1 Parameters of the internal gear pair

Parameters	External gear	Internal gear
Number of teeth	30	70
Module (mm)	3	3
Teeth width (mm)	25	25
Pressure angle (°)	20	20
Base radius (m)	0.042	0.099
Helical angle (°)	0	0
Young modulus (N/mm^2)	2×10^5	
Poisson's ratio	0.3	

Table 2 Profile shift coefficients of the internal gear pair

Case No.		A	B	C	D	E
I (x_2–x_1=0)	x_1	–0.33	–0.20	0	0.50	0.99
	x_2	–0.33	–0.20	0	0.50	0.99
	CR	2.19	2.10	1.96	1.69	1.49
II (x_2–x_1=0.21>0)	x_1	–0.33	–0.20	0	0.5	0.99
	x_2	–0.12	0.01	0.21	0.71	1.20
	CR	2.08	1.996	1.89	1.66	1.48
III (x_2–x_1=–0.19<0)	x_1	–0.33	–0.20	0	0.5	0.99
	x_2	–0.52	–0.39	–0.19	0.31	0.80
	CR	2.32	2.19	2.03	1.71	1.48

Note: *CR* indicates the contact ratio of the gear pair given in Table 1 with different profile shift coefficients.

tacting with each other at the pitch point. The negative and positive angular positions represent the mesh point ahead of and lag behind the pitch point, respectively, when the external gear is the driving component. The rotational angle of the external gear corresponding to the curves in these figures represents the entire mesh processing from tooth root to tip of the external gear. While for the internal gear, the mesh point moves from its tooth tip to root along the involute curve.

3.1 Effect of tooth profile shift coefficient on gear tooth compliance

Based on the analysis on the effect of the tooth profile shift in section 2, the profile shifted gear will change its tooth thickness, the center distance, the radius of the tip, pitch and root circles, as well as the working segment of the involute tooth profile. It can be predicted that the compliances of the tooth and the fillet foundation are likely to be changed if the profile of the gear is shifted, thus leading to the variation of the tooth stiffness and further the mesh stiffness.

The bending, shear, and axial compressive compliances of the gear pairs in Case I are extracted and shown in Figure 3. It can be seen that, for both external and internal gears, the compliance curve will move towards the positive direction as the increase of the tooth profile shift coefficient, which indicates that the mesh point will lag more behind the pitch point of the internal gear pair. At the same time, the rotational angle range of the external gear corresponding to the whole process when a specified tooth is in engagement will shrink as the growth of the tooth profile shift coefficient, namely, the contact ratio will become smaller as shown in Table 2. Another phenomenon can be observed in Figure 3(a) and (c) that the bending and shear compliances of the external gears with an external force applied at the tip circle along the line of action will decrease firstly, and then increase as the growth of the tooth profile shift coefficient. While for the internal gear tooth, its bending and shear compliances for the position at the tooth tip will decrease with the increase of the tooth profile shift coefficient, which are shown in Figure 3(b) and (d). However, the axial compressive compliances of the tooth tip, whatever for external

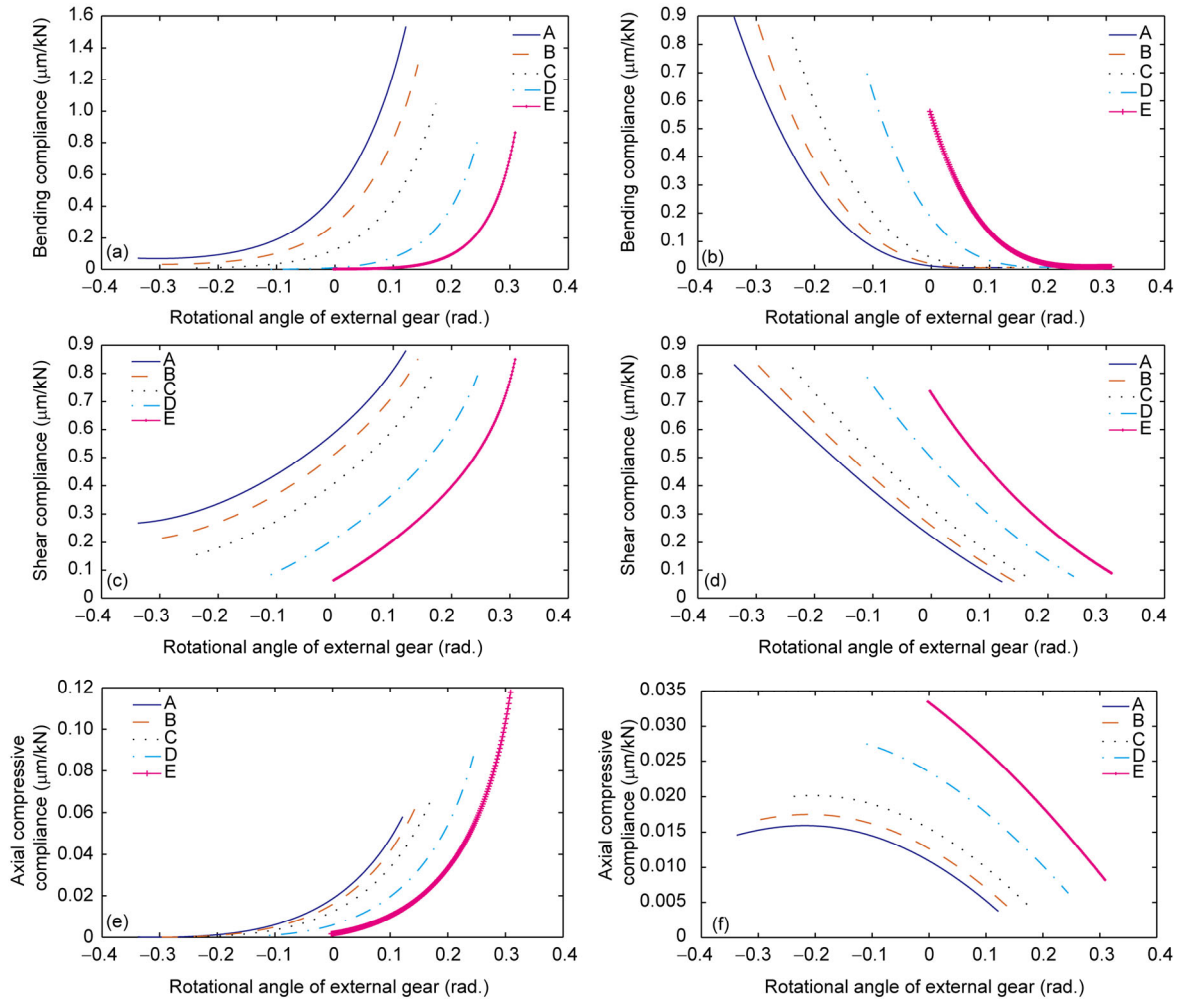

Figure 3 (Color online) Compliance of gear teeth in Case I: (a), (c), and (e) for external gears, and (b), (d), and (f) for internal gears.

or internal gears, will increase with the tooth profile shift coefficient, which are shown in Figure 3(e) and (f). These results can be interpreted by the characteristics of a profile shifted gear tooth. If a gear has a positive profile shift, its radius of root circle and tip circle will enlarge which results in the tooth root and tip moving away from the gear center. For this case, the tooth root will become thicker while the tooth tip thinner compared with the standard gear tooth. While, if a gear has a negative tooth profile shift, it has an inverse change. At the same time, the mesh force components parallel with and perpendicular to center plane around which the tooth is symmetric will vary as the gear rotation. This will also affect the calculation of tooth compliance. Consequently, some of the factors will enhance the tooth compliance while others will reduce. Whether the tooth compliance increases or decreases is determined by which factor plays the major role.

The parameters for the tooth fillet foundation will be altered if the gear tooth profile is shifted. How the tooth profile shift affects the tooth compliance is demonstrated in Figure 4 where it can be seen that the compliance of the external gear tooth with an external force applied to its tip along the line of action will decrease as the growth of the tooth profile shift coefficient. In other word, the tooth fillet foundation of the gear with a bigger profile shift coefficient will become stiffer, which is due to fact that the gear has a thicker tooth root and smaller force component perpendicular to the tooth symmetric center line. In this paper, the effect of the tooth profile shift on the fillet foundation of an internal gear is not considered, and this is expected to be studied in the future work.

Then the tooth stiffness can be easily obtained by eq. (24) if the tooth bending, shear, axial compressive, and tooth fillet foundation compliances have been calculated.

The calculated results of the external and internal gear tooth stiffness for the Case I in Table 2 are displayed in Figure 5. It can be seen that the position for the curves will shift towards top right (see Figure 5(a)), which indicates that the tooth stiffness of the external gear has the tendency to increase with growth of the tooth profile shift coefficient. While for the internal gear tooth stiffness curves, their positions will shift towards lower right which means it has a reduction tendency (see Figure 5(b)). An observation can be gained that the tooth stiffness amplitude of the internal gear is much greater than that of the external gear. This is due to that the rim flexibility of the internal gear is not considered in this paper. After obtaining the tooth stiffness of the internal gear pair, the single- and multi-tooth mesh stiffness can be calculated by eq. (26), which is going to be introduced in subsection 2.2.

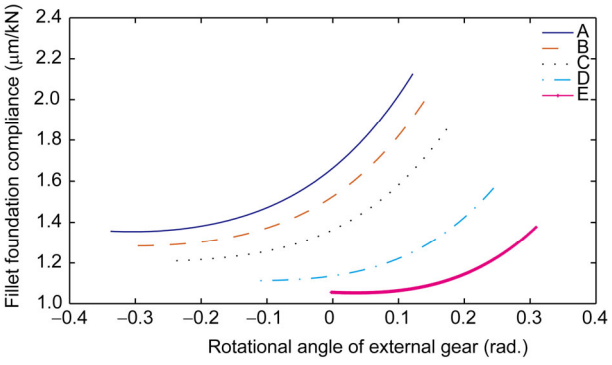

Figure 4 (Color online) Fillet foundation compliance of external gears.

3.2 Effect of tooth profile shift coefficient on mesh stiffness

The calculated single- and multi-tooth mesh stiffness results of the internal gear pair with different tooth profile shift coefficients given in Table 2 are represented in Figures 6–9. In these figures, the horizontal axis indicates the rotational angle of the external gear when a concerned tooth is in engagement. As can be seen in Figures 6–8, the mesh stiffness curves are shifted to the right side as the increase in the tooth profile shift coefficient when a fixed center distance of the gear pair is given. That is to say the phase of the mesh stiffness curve will vary with different profile shift coefficients, which can be observed clearly in the diagrams of multi-tooth mesh stiffness (e.g. Figures 6(b), 7(b) and 8(b)). Simultaneously, the amplitude of the single-tooth mesh stiffness has a trend to increase with the growth of the tooth profile shift coefficient. Consequently, the dynamic responses of the internal gear transmission system are likely to be affected by the tooth profile shift.

Another noticeable phenomenon can be also observed in Figures 6–8 that the contact ratio will be drastically reduced as the increase of the tooth profile shift coefficient under a given fixed center distance of the internal gear pair. The contact ratio is reduced from a value bigger than 2 to that lower than 2 for all the three cases given in Table 2, e.g. from case B to C in Figure 6(b). All these discrepancies in the mesh stiffness curves of the internal gear pair with shifted tooth profile are contributed from the variation of the geometric parameters caused by the tooth profile shift, such as the tooth thickness distribution from the tooth tip to root, diametrical change of the tip circles.

However, the discrepancies in the mesh stiffness curves of the internal gear pair with different center distances are hard to observe in Figures 6–8. In order to reveal the effect of tooth profile shift coefficient under different center distances on the mesh stiffness, case C is designed in Table 2. The corresponding results for all the three cases, namely cases I, II and III, are displayed in Figure 9. It can be observed that a bigger center distance (case II) will push the mesh stiffness curve to the left side relative to the standard case (case I), while a shorter center distance will make it to move to the right side (case III). Namely, the phase of the mesh stiffness will be ahead of the standard case when the gear center distance is enlarged by tooth profile shift, on the

contrary, it will be lag behind that of the standard case if the gear center distance is shortened.

Based on the analysis above, it has been known that the contact ratio and the single-tooth mesh stiffness will vary with the tooth profile shift, and its amplitude of variation is determined by the extent of the profile shift. This means

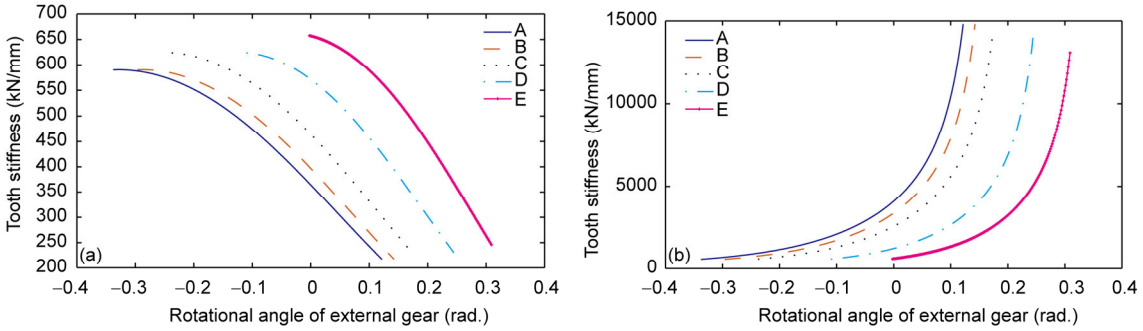

Figure 5 (Color online) Tooth stiffness of internal gear pair in Case I: (a) external and (b) internal gears.

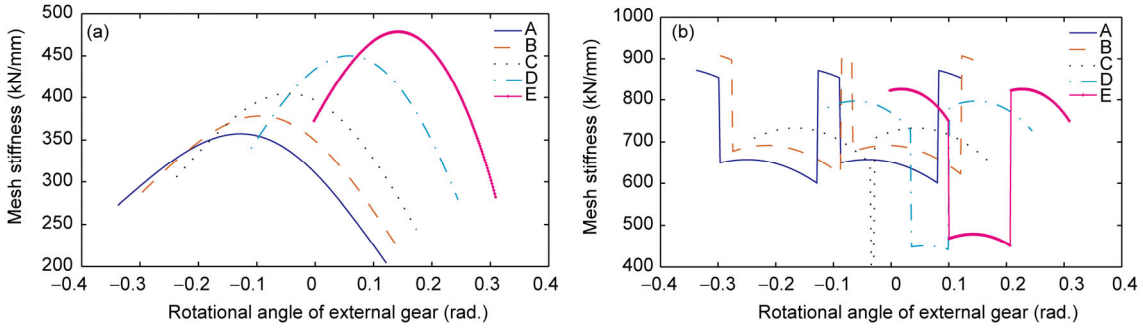

Figure 6 (Color online) Mesh stiffness curves of internal gear pair for Case I: (a) single- and (b) multi-tooth engagements.

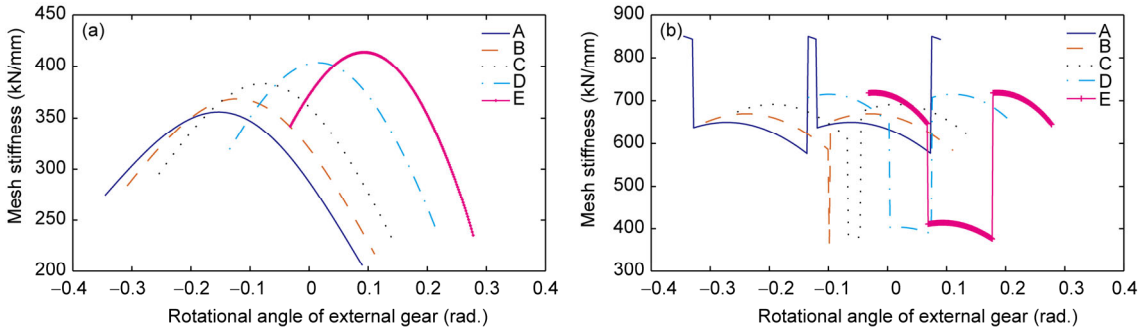

Figure 7 (Color online) Mesh stiffness curves of internal gear pair for Case II: (a) single- and (b) multi-tooth engagements.

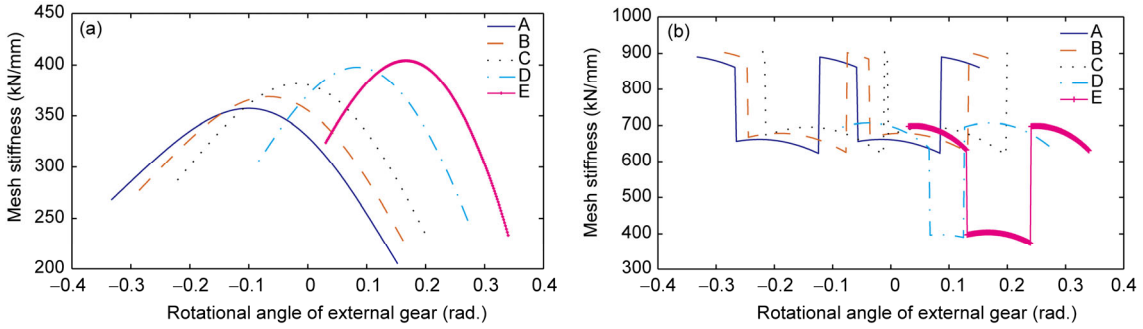

Figure 8 (Color online) Mesh stiffness curves of internal gear pair for Case III: (a) single- and (b) multi-tooth engagements.

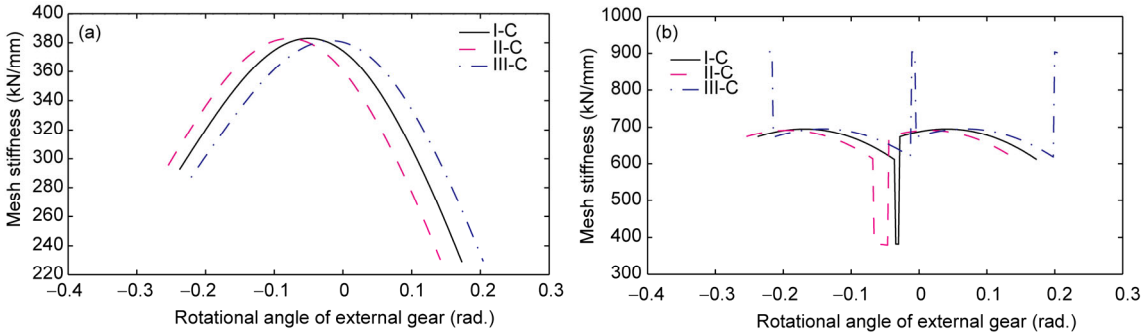

Figure 9 (Color online) Mesh stiffness curves of internal gear pair: (a) single- and (b) multi-tooth engagements.

that the load capacity of the gear teeth will change with the tooth profile shift. As an example, the load sharing ratios for the internal gear pairs in case I are extracted and exhibited in Figure 10. It can be seen that, in general, the value of the load sharing ratio will increase with a larger profile shift coefficient. Under this condition, the load carried by one teeth pair will increase if a constant external torque is applied to the gear pair. Thus, the characteristics of the bending and contact fatigue are likely to vary with the tooth profile shift.

In addition, in order to learn further the effect of the tooth profile shift coefficient on the mesh stiffness of the internal gear pair, some statistical indicators, such as the root mean square (RMS) representing its variation level, the mean value, and the peak-peak value, are adopted here. The mean, RMS, and peak-peak values are calculated, respectively, as [5,42]

$$\bar{x} = \frac{1}{N}\sum_{n=1}^{N} x_s(n), \tag{28}$$

$$x_{\mathrm{RMS}} = \sqrt{\frac{1}{N}\sum_{n=1}^{N}(x_s(n)-\bar{x})^2}, \tag{29}$$

$$x_{\mathrm{p\text{-}p}} = \max(x_s(n)) - \min(x_s(n)), \text{where } n = 1,2,\cdots,N, \tag{30}$$

where x_s denotes the analyzed data with the length of N, and it represents the mesh stiffness of the internal gear pair here.

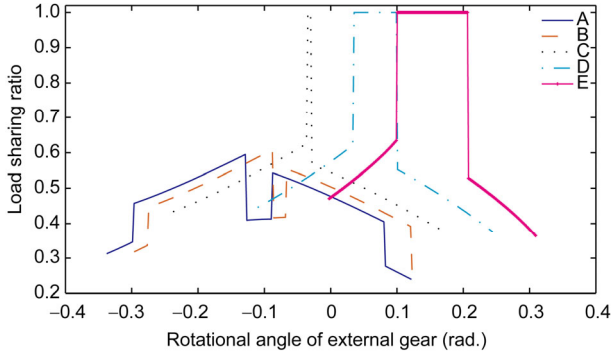

Figure 10 (Color online) Load sharing ratio of the internal gear with different tooth profile shift in Case I.

The symbols, namely $\bar{x}$, x_{RMS}, and $x_{\mathrm{p\text{-}p}}$, stand for the mean, RMS, and peak-peak values, respectively. The operators max and min are used to select the maximum and minimum values.

The results showing the effect of the tooth profile shift coefficients on the single-tooth mesh stiffness (SMS) and the multi-tooth mesh stiffness (MMS) at the statistical point of view are given in Figure 11. It can be seen that the mean value of the SMS will increase with the tooth profile shift coefficient varying from smaller to bigger values, while an inverse tendency can be found for that of the MMS which will increase when the center distance of the internal gear pair is reduced. Besides, it can be also found that the peak-peak value for both the SMS and MMS will increase as the growth of the tooth profile shift coefficient, while they are hardly affected by the variation of the center distance of the internal gear pair. The relationship found for the peak-peak value versus tooth profile shift coefficient is also suitable for the RMS value of the SMS. However, the RMS curve is influenced greatly by the tooth profile shift coefficient and the center distance of the internal gear pair. The minimum value of the RMS indicator is observed when the contact ratio of the gear pair is approaching an integer. It should be noted that the mean, the peak-peak, and the RMS values of MMS are calculated within a mesh cycle.

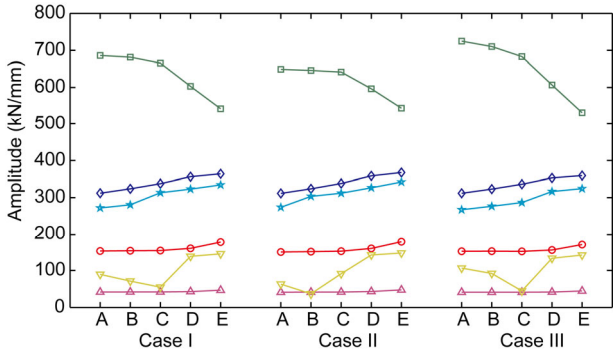

Figure 11 (Color online) Statistical indicators of the internal gear mesh stiffness with different profile shift coefficients with: $\bar{x}$ of the SMS, $\bar{x}$ of the MMS, $x_{\mathrm{p\text{-}p}}$ of the SMS, $x_{\mathrm{p\text{-}p}}$ of the MMS, x_{RMS} of the SMS, x_{RMS} of the MMS.

From the analysis on the mesh stiffness of an internal gear pair above, it can be predicted that the dynamic responses of an internal gear pair is likely to be changed bythe gear tooth profile shift based on the fact that the tooth profile shift will alter the shape, the mean value, and the peak-peak value of the mesh stiffness. This may offer the possibilities for the optimization of the tooth profile shift coefficient at the view point of vibration and noise even if the tooth profile shift is mainly employed to prevent tooth undercut, adjust the center distance, eliminate interference, and equalize specific sliding and tooth bending fatigue life and so on.

4 Conclusions

An extended analytical model for mesh stiffness calculation of an internal spur gear pair with shifted tooth profile has been developed in this paper to investigate the effect of the gear tooth profile shift coefficient on the gear mesh stiffness excitations. How the tooth profile shift influences the design parameters of the gear teeth and further the mesh stiffness of an internal gear pair is analyzed theoretically. Three groups of individual internal gear pairs, namely the center distance of the profile shifted internal gear pair is equal to, larger and smaller than that of its standard form, are selected to demonstrate the effect of the gear tooth profile shift on the gear tooth compliance, the mesh stiffness, and the load sharing ratio. The results indicate that tooth profile shift has an obvious effect on the tooth compliance, the mesh stiffness, and the load sharing ratio, including their amplitude, shape and initial phase. These influences could be attributed to the variations of the tooth thickness distribution along tooth height, radius of the tip and root circles, and the contact ratio caused by the tooth profile shift. This promotes that achievement of optimization on the tooth profile shift coefficient at the vibration point of view is possible together with the design requirements on the selection of tooth profile shift coefficients. This is expected to be studied in the future work. Although the mesh stiffness calculation model is established based on an internal spur gear pair, it can be extended easily to involve the mesh stiffness calculation of external gear pairs with tooth profile shift.

This work was supported by the National Natural Science Foundation of China (Grant Nos. 51405400 & 51375403), the Fundamental Research Funds for the Central Universities (Grant Nos. 2682015ZD12 & 2682016CX125), and the Fundamental Research Funds for State Key Laboratory of Traction Power (Grant Nos. 2015TPL_T14 & 2014TPL_T10). The authors also thank the anonymous reviewers for their valuable comments and suggestions to improve this paper.

1 Hidaka T, Terauchi Y, Ishioka K. Dynamic behavior of planetary gear-2nd report: displacement of sun gear and ring gear. Bull JSME, 1976, 19: 1563–1570
2 Hidaka T, Terauchi Y, Nohara M, et al. Dynamic behavior of planetary gear-3rd report: displacement of ring gear in direction of line of action. Bull JSME, 1977, 20: 1663–1672
3 Karas F. Elastische Formänderung und Lastverteilung beim Doppeleingriff gerader Stirnradzähne. V.D.I. Forschh. 1941, 406: 1–17
4 Chen Z G, Shao Y M. Dynamic simulation of planetary gear with tooth root crack in ring gear. Eng Fail Anal, 2013, 31: 8–18
5 Chen Z G, Shao Y M. Dynamic simulation of spur gear with tooth root crack propagating along tooth width and crack depth. Eng Fail Anal, 2011, 18: 2149–2164
6 Chen Z G, Shao Y M. Mesh stiffness of an internal spur gear pair with ring gear rim deformation. Mech Mach Theory, 2013, 69: 1–12
7 Chen Z G, Shao Y M, Su D Z. Dynamic simulation of planetary gear set with flexible spur ring gear. J Sound Vib, 2013, 332: 7191–7204
8 Satoshi O D A, Miyachika K. Root stress of thin-rimmed internal spur gear supported with pins. JSME Int J, 1987, 30: 646–652
9 Kahraman A, Kharazi A A, Umrani M. A deformable body dynamic analysis of planetary gears with thin rims. J Sound Vib, 2003, 262: 752–768
10 Kahraman A. Load sharing characteristics of planetary transmissions. Mech Mach Theory, 1994, 29: 1151–1165
11 Singh A. Load sharing behavior in epicyclic gears: physical explanation and generalized formulation. Mech Mach Theory, 2010, 45: 511–530
12 Singh A. Application of a system level model to study the planetary load sharing behavior. ASME J Mech Design, 2005, 127: 469–476
13 Sun T, Hu H. Nonlinear dynamics of a planetary gear system with multiple clearances. Mech Mach Theory, 2003, 38: 1371–1390
14 Lin J, Parker R G. Analytical characterization of the unique properties of planetary gear free vibration. T ASME J Vib Acoust, 1999, 121: 316–321
15 Lei Y G, Lin J, Zuo M J, et al. Condition monitoring and fault diagnosis of planetary gearboxes: A review. Measurement, 2014, 48: 292–305
16 Chaari F, Fakhfakh T, Haddar M. Analytical modelling of spur gear tooth crack and influence on gearmesh stiffness. Eur J Mech A-Solids, 2009, 28: 461–468
17 Weber C. The deformation of loaded gears and the effect on their load carrying capacity. Sponsored research, British Department of Science and Industrial Research, London, 1949
18 Cornell R W. Compliance and stress sensitivity of spur gear teeth. ASME J Mech Design, 1981, 103: 447–459
19 O'Donnell W J. Stress and deflection of built-in beams. ASME Paper No. 62-WA-16, 1974
20 Omar F K, Moustafa K A F, Emam S. Mathematical modeling of gearbox including defects with experimental verification. J Vib Control, 2011, 18: 1310–1321
21 Yang D C H, Lin J Y. Hertzian damping, tooth friction and bending elasticity in gear impact dynamics. J Mech T Auto Design, 1987, 109: 189–196
22 Tian X. Dynamic Simulation for system response of gearbox including localized gear faults. Dissertation of Master Degree. Alberta: University of Alberta, Edmonton, 2004
23 Tian X, Zuo M J, Fyfe K R. Analysis of the vibration response of a gearbox with gear tooth faults. In: The 2004 ASME International Mechanical Engineering Congress and Exposition, Anaheim, California USA, 2004: 785–793
24 Wu S, Zuo M J, Parey A. Simulation of spur gear dynamics and estimation of fault growth. J Sound Vib, 2008, 317: 608–624
25 Mohammed O D, Rantatalo M, Aidanpää J. Improving mesh stiffness calculation of cracked gears for the purpose of vibration-based fault analysis. Eng Fail Anal, 2013, 34: 235–251
26 Liang X H, Zuo M J, Patel T H. Evaluating the time-varying mesh stiffness of a planetary gear set using the potential energy method. P I Mech Eng C-J Mec, 2014, 228: 535–547
27 Liang X H, Zuo M J, Pandey M. Analytically evaluating the influence of crack on the mesh stiffness of a planetary gear set. Mech Mach Theory, 2014, 76: 2014

28 Chen Z G, Shao Y M. Mesh stiffness calculation of a spur gear pair with tooth profile modification and tooth root crack. Mech Mach Theory, 2013, 62: 63–74
29 Wang Q, Hu P, Zhang Y, et al. A model to determine mesh characteristics in a gear pair with tooth profile error. Adv Mech Eng, 2014: 1–10
30 AGMA 913-A98. Method for specifying the geometry of spur and helical gears, 1998
31 Mirica R F, Dobre G. On the distribution of the profile shift coefficients between mating gears in the case of cylindrical gear. In: 12th IFToMM World Congress, Besançon, 2007
32 Hu Y M, Shao Y M, Chen Z G, et al. Transient meshing performance of gears with different modification coefficients and helical angles using explicit dynamic FEA. Mech Syst Signal Pr, 2011, 25: 1786–1802
33 ISO/TR 4467, Addendum modification of the teeth of cylindrical gears for speed-reducing and speed-increasing gear pairs, 1982
34 DIN 3992, Profilverschiebung bei Stirnrädern mit Aussenverzahnung, 1964
35 Ristivojević M, Lazović T, Vencl A. Studying the load carrying capacity of spur gear tooth flanks. Mech Mach Theory, 2013, 59: 125–137
36 Marimuthu P, Muthuveerappan G. Optimum profile shift estimation on direct design asymmetric normal and high contact ratio spur gears based on load sharing. Procedia Engineering, 2014, 86: 709–717
37 Abderazek H, Ferhat D, Atanasovska I, et al. A differential evolution algorithm for tooth profile optimization with respect to balancing specific sliding coefficients of involute cylindrical spur and helical gears. Adv Mech Eng, 2015, 7: 1–11
38 Rajesh A R, Gonsalvis J, Venugopal K A. Load sharing analysis of bending strength in altered tooth-sum gears operating between a standard center distance and module. Eur J Eng Tech, 2015, 3: 50–61
39 Shiau T N, Chang J R, Huang K H, et al. Nonlinear dynamic analysis of a multi-gear train with time-varying mesh stiffness including modification coefficient effect. In: Proceedings of ASME Turbo Expo 2011, June 6-10, 2011, Vancouver, British Columbia, Canada
40 Ma H, Pang X, Feng R, et al. Evaluation of optimum profile modification curves of profile shifted spur gears based on vibration responses. Mech Syst Signal Pr, 2016, 70–71: 1131–1149
41 Ma H, Feng R, Pang X, et al. Effects of tooth crack on vibration responses of a profile shifted gear rotor system. J Mech Sci Tech, 2015, 29: 4093–4104
42 Lebold M, McClintic K, Campbell R, et al. Review of vibration analysis methods for gearbox diagnostics and prognostics. In: Proceedings of the 54th meeting of the society for machinery failure prevention technology, Virginia Beach, VA, 2000. 623–634